Cerebral Cortex January 2011;21:134–144
doi:10.1093/cercor/bhq070
Advance Access publication May 3, 2010

Lrp12/Mig13a Reveals Changing Patterns of Preplate Neuronal Polarity during Corticogenesis that Are Absent in *Reeler* Mutant Mice

Stephanie Schneider[1], Alexandra Gulacsi and Mary E. Hatten

Laboratory of Developmental Neurobiology, The Rockefeller University, New York, NY 10065, USA

[1]Current address: Institute for Zoology, University of Heidelberg, 69120 Heidelberg, Germany

Address correspondence to Mary E. Hatten. Email: hatten@mail.rockefeller.edu.

During corticogenesis, the earliest generated neurons form the preplate, which evolves into the marginal zone and subplate. *Lrp12/Mig13a*, a mammalian gene related to the *Caenorhabditis elegans* neuroblast migration gene *mig-13*, is expressed in a subpopulation of preplate neurons that undergo ventrally directed tangential migrations in the preplate layer and pioneer axon projections to the anterior commissure. As the preplate separates, *Lrp12/Mig13a*-positive neurons polarize in the radial plane and form a pseudocolumnar pattern, prior to moving to a deeper position within the emerging subplate layer. These changes in neuronal polarity do not occur in *reeler* mutant mice, revealing the earliest known defect in *reeler* cortical patterning and suggesting that the alignment of preplate neurons into a pseudolayer facilitates the movement of later-born radially migrating neurons into the emerging cortical plate.

Keywords: corticocortical connections, *Lrp12/Mig13a*, neuronal polarity, preplate development, *Reeler*

Introduction

The emergence of the laminar architecture of the mammalian forebrain depends on the spatiotemporal pattern of neurogenesis, migration of postmitotic neurons (Caviness and Sidman 1973; Zecevic et al. 1999; Nadarajah et al. 2001; Molnar et al. 2006), formation of transverse zones of transient neurons (preplate, cortical plate, marginal zone, and subplate) (Caviness 1982; Allendoerfer and Shatz 1994; McConnell et al. 1994; Del Rio et al. 2000; Zecevic and Rakic 2001), and positioning of the principal classes of cortical neurons into neuronal layers. Although these basic steps of corticogenesis are conserved among mammalian species, studies on human and nonhuman primate corticogenesis indicate differences in the period of neurogenesis, the temporal gradient of maturation across the hemisphere, and cellular complexity of the transient cell layers (Bystron et al. 2008). In the mouse, the earliest neurons generated in the ventricular zone (VZ) of the dorsal telencephalon become postmitotic on, or before, the eleventh day of gestation (E11). These early-born polymorphic neurons complete their migrations by E13 and settle in a narrow laminar zone, the preplate (Caviness 1982; Kostovic and Rakic 1990; Wood et al. 1992; McConnell et al. 1994; Del Rio et al. 2000; Zecevic and Rakic 2001). The preplate, now recognized as the initial zone of postmigratory neurons and neuropil, forms between the VZ and the pial surface of the dorsal telencephalon (Bystron et al. 2008). Between E13–E15 in the mouse, radially migrating neurons pattern a second transient layer in the middle of the preplate, the cortical plate. As the cortical plate forms, preplate neurons simultaneously segregate into a superficial marginal zone containing Cajal–Retzius cells and a deeper layer, the subplate (Caviness 1982; Wood et al. 1992; McConnell et al. 1994; Del Rio et al. 2000; Molnar et al. 2006).

Studies on the genetics of cortical development underscore the importance of preplate separation to the development of laminar cytoarchitectonics. During corticogenesis in *reeler* mutant mice, the segregation of preplate neurons into 2 zones and formation of the cortical plate does not occur and subsequent cortical lamination fails (Caviness and Rakic 1978; Goffinet 1984; Tissir and Goffinet 2003). The *Reelin (Reln)* protein (RELN) binds to 2 members of the lipoprotein receptor family, the very low-density lipoprotein receptor (*VLDLR*) and the apolipoprotein E receptor type 2 (*APOER2*) (D'Arcangelo et al. 1995; Trommsdorff et al. 1999; Herz and Bock 2002; Tissir and Goffinet 2003). Mice lacking *Vldlr* and *ApoER2* have cortical malformations similar to a *reeler* phenotype. RELN signaling activates nonreceptor tyrosine kinases of the Src and Fyn families, leading to tyrosine phosphorylation of the intracellular adapter *DAB1* (Howell et al. 1997; Jossin et al. 2003) and phosphatidylinositol 3-kinase (Jossin and Goffinet 2007). Genetic ablation of *Src* and *Fyn* kinases or inhibitors of *Src* family kinases (SFKs) also lead to defects in the orientation and lamination of cortical neurons (Jossin et al. 2003; Kuo et al. 2005).

The overall plan of cortical connectivity includes the formation of reciprocal connections between the cortex and the thalamus and corticocortical connections between the cerebral hemispheres (McConnell et al. 1994; Xie et al. 2002; Richards et al. 2004; Price et al. 2006). These projections are pioneered by axons of transient populations of neurons in the preplate, and later, by neurons in the subplate (De Carlos and O'Leary 1992; McConnell et al. 1994). Since many local cues and signaling pathways that affect axon navigation and cell migration are evolutionarily conserved, one approach to discovering novel regulators of cortical development is to identify vertebrate genes whose invertebrate homologs affect normal development (Kee et al. 2007). In *Caenorhabditis elegans*, 3 classes of neurons (anterior lateral microtubule cell, canal-associated neurons, and hermaphrodite specific neuron) and one line of neuroblasts, Q cells and their descendants, undergo extensive migrations during central nervous system (CNS) development (Blelloch et al. 1999; Shakir and Lundquist 2005). QR neuroblasts migrate toward the anterior by a mechanism that involves instructive changes in the level of expression of the transmembrane protein MIG-13 (Sym et al. 1999). In this study, we identify *Lrp12/Mig13a*, a mammalian gene related to *mig-13*, as a novel marker for a distinct subpopulation of preplate neurons. To map the pattern of gene expression, we generated lines of bacterial artificial chromosome transgenic mice that express the enhanced green fluorescent protein (Egfp) reporter gene under the control of

the native *Lrp12/Mig13a* locus [*Tg(Lrp12/Mig13a-Egfp)*] (Gong et al. 2003). In these mice, *Lrp12/Mig13a* expression is restricted to a transient population of cells in the preplate, which segregate into the subplate during formation of the cortical plate. The present studies reveal a novel series of cell movements that orient the polarity of *Lrp12/Mig13a*-expressing neurons and their axons just prior to cortical plate assembly. These changes do not occur in *reeler* mutant mice or after perturbation of the RELN signaling pathway in wild-type mice. Our results suggest an earlier defect than previously recognized in *reeler* corticogenesis, which involves defects in local cell movements needed to align into a pseudolayer rather than an arrest of neuronal migration along glial fibers.

Materials and Methods

Animal Breeding and Genotyping

Tg(Lrp12/Mig13a-Egfp) transgenic mice [*CD-1-Tg(RP23-181D20)BG31Gen*] were generated as described previously (Gong et al. 2003). The *reeler* mutation, gene symbol *rl or Reln,* is maintained on *B6C3Fea/a* hybrid mouse strain (Jackson Laboratory). To express *Lrp12/Mig13a-Egfp* in *rl/rl* mutant mice, we crossed a male *Tg(Lrp12/Mig13a-Egfp)* with a female *B6C3Fea/a-Reln^{rl}/J* mouse (Jackson Laboratory [stock number 000235]) and intercrossed F_1 offspring to generate *B6C3FeTg(Lrp12/Mig13a-Egfp)a-Reln^{rl}/a-Reln^{rl}* mice. The genotype of *B6C3FeTg(Lrp12/Mig13a-Egfp)a-Reln^{rl}/a-Reln^{rl}* and *B6C3Fe-Tg(Lrp12/Mig13a-Egfp)*a/J embryos was confirmed by polymerase chain reaction (PCR) analysis for Egfp and *Reln^{rn}* as described (D'Arcangelo et al. 1996; Gong et al. 2003). All animal procedures were performed in accordance with institutional guidelines.

BrdU Birthdating of Lrp12/Mig13a-Positive Cells

The pregnant female was injected intraperitoneally with thymidine analog 5′-bromo-2′-deoxyuridine (BrdU) (5 mg/g body weight) at 24-h intervals between the 10th (El0.5) and 12th (E12.5) days of gestation. Animals were killed 1–3 days later by an overdose of Pentobarbital (Nembutal; Abbott), and embryos were removed by laparotomy. The embryos/brains were fixed and immunostained with antibodies against BrdU and enhanced green fluorescent protein (EGFP) as described below to correlate *Lrp12/Mig13a* expression with neurogenesis.

Immunohistochemistry

Tg(Lrp12/Mig13a-Egfp) embryos or embryonic brains were dissected in phosphate-buffered saline (PBS) (4 °C), fixed in paraformaldehyde (4%, 4 °C, 1–3 h), immersed in sucrose (30%, 4 °C, overnight), embedded in Neg-50 (Richard-Allan Scientific), and sectioned (20 μm) with a Microm Model HM 500 M Cryostat (GMI, Inc.). Nonspecific immunostaining was blocked by pretreating with normal donkey serum (5% in PBS containing 0.1% Triton-X-100; Jackson ImmunoResearch Laboratories, Inc.). Primary and secondary antibody staining was carried out at 4 °C overnight. The primary antibodies used in this study were anti-GFP rabbit polyclonal antibody (1:2000, Molecular Probes), anti-GFP antibody (sheep polyclonal, 1:250; Biogenesis), anti-LRP12/MIG13A antibody (rabbit polyclonal, 1:50) (Schneider S, Gulacsi A, Gong S, Ayad N, Hatten ME, in preparation), anti-TAG-1 antibodies (mouse monoclonal, Dr Jane Dodd, Columbia University, NY), anti-L1 (mouse monoclonal IgG, 324, 1:20; Dr J. Trotter, University of Mainz, Germany), anti-CALB1 antibody (rabbit polyclonal, 1:1000; Swant), anti-RELN antibody (mouse monoclonal IgG, clone G10, 1:1000; Chemicon/Millipore Biosciences Division, Danvers, MA), anti-CALB2 antibodies (rabbit polyclonal, 1:1000) (Swant), anti-BrdU antibodies (mouse monoclonal IgG, 1:100, Becton Dickson Biosciences), anti-MAP2 antibodies (mouse monoclonal IgG, clone SMI 52, Covance), and anti-GM130 antibodies (mouse monoclonal IgG, BD Biosciences). Secondary antibodies were purchased from Jackson ImmunoResearch and Molecular Probes (Invitrogen Corp.). Nuclei were visualized using 4′,6-diamidino-2-phenylindole (DAPI) (Sigma) or DRAQ5 (Axxora LLC.). Double staining for EGFP and BrdU was performed by immunostaining for EGFP, as described above, postfixing, treating with 4 N HCl/0.5% Tween20 (20 min), and then with 0.1 M Borax buffer pH 8.5 (5 min), and staining with anti-BrdU primary antibody (mouse monoclonal IgG, 1:100, Becton Dickson Biosciences) and anti-mouse secondary antibody as above. Images were acquired using an Axioscope 200 inverted microscope (Zeiss) with a LSM510 confocal laser scanhead (Carl Zeiss Microimaging, Inc.).

In Situ Hybridization

Embryos were fixed with paraformaldehyde and immersed in sucrose (30%, 4 °C, overnight), after which 60-μm sections were generated with a Leica RM2265 microtome (Leica Microsystems, Inc.). Hybridization and detection were performed as described (Schaeren-Wiemers and Gerfin-Moser 1993). The *Lrp12/Mig13a* in situ probe was amplified with the following primers: sense primer 5′-GTCAGTTGATCGCTCAGGG-3′ and antisense primer 5′-GGACAGATACACAAGACCTC-3′.

PP2 Treatment of Tg(Lrp12/Mig13a-Egfp) Neocortical Slice Cultures

To assay the effects of SFK inhibitor PP2 (Calbiochem) on *Lrp12/Mig13a*-positive preplate cells, coronal slices (250 μm) of E12.5 *Tg(Lrp12/Mig13a-Egfp)* mouse neocortex, generated with a Leica VT100S vibrating blade microtome (Leica Microsystems, Inc.), were cultured in 35% Eagle's Basal Medium, 35% L15, 25% complete Hank's balanced salt solution, 20 mM D-glucose, 1 mM L-Glutamine, 10 mM Hepes, 1× Pen/Strep, 5% heat-inactivated horse serum. For SFK inhibition, E12.5 *Tg(Lrp12/Mig13a-Egfp)* cortical slices were cultured in medium supplemented with dimethyl sulfoxide with or without 10 μM PP2.

Imaging of Preplate Neuron Motility

Coronal slices (250 μm) of E12.5 or E13.5 *Tg(Lrp12/Mig13a-Egfp)* neocortex were maintained at 37 °C in a Warner environmental imaging chamber (Warner Instruments) for 7–15 h. Time-lapse images were acquired with a NLO LSM 510 multiphoton microscope (Zeiss) equipped with a Coherent Chameleon multiphoton 870 nm laser, Zeiss LSM software, Imaris (Bitplane Scientific Solutions) and ImageJ. For Supplementary Movie 1, we used Photoshop CS3 to isolate a series of time-lapse images of a single migrating cell by hand, after which we used Final Cut Pro to sequence the images chronologically and add text, and QuickTime conversion software to export the resulting movie into MPEG-4 format. ImageJ software (http://rsb.info.nih.gov/ij/) was used to determine the trajectory and speed of migration of *Lrp12/Mig13a*-positive neurons in *Tg(Lrp12/Mig13a-Egfp)* tissue slices.

Measuring Neuronal Polarity with Anti-GM130 Antibody Staining

To visualize the nucleus and Golgi apparatus of *Lrp12/Mig13a*-postive neurons in coronal cryosections (20 μm) of *Tg(Lrp12/Mig13a-Egfp)*, *B6C3Fe-Tg(Lrp12/Mig13a-Egfp)*a/J, or B6C3Fe*Tg(Lrp12/Mig13a-Egfp)a-Reln^{rl}/a-Reln^{rn}* embryos, embryonic brains were immunostained with anti-EGFP and anti-GM130 antibodies and counterstained with DAPI. To measure the polarity of preplate neurons relative to the neuroaxis, we drew a line from the center of the DAPI-stained nucleus through the center of the GM130-positive Golgi apparatus. ImageJ software was used to score and bin the orientation of *Lrp12/Mig13a*-positive preplate cells as illustrated in Figures 7*e* and 8*e* and Supplementary Figure 8*e*. To measure the polarity of *Lrp12/Mig13a*-postive neurons in slice cultures of E12.5 neocortex, cultured for 0div or 2div, we fixed the slices and resectioned them (20 μm) using a cryostat, immunostained the slices with anti-EGFP and anti-GM130 antibodies and counterstained them with DAPI. The orientation (polarity) of *Lrp12/Mig13a*-postive cells relative to the neuroaxis was measured as described above.

SMARTpool siRNA Silencing Studies

HEK 293T cells were cotransfected with Flag-tagged full-length *Lrp12/Mig13a* cDNA and control nontargeting small interfering (siRNA) pool (Thermo Scientific Dharmacon siGENOME Control Pool, Non-Targeting no. 2, Cat no. D-001206-14-05) or *Lrp12/Mig13a* siRNA pool (Thermo

Scientific Dharmacon siGENOME SMARTpool, Mouse C820005L12RIK, Cat no. M-055299-00), using Lipofectamine 2000. Five microgam of DNA/7.5 μL of 20 μM (2 μg) siRNA pool/250 μL of Dulbecco's Modified Eagle's Medium (DMEM) were mixed with 7.5 μL of Lipofectamine 2000/250 μL of DMEM and added to one well of a 6-well plate. Lysates were harvested 24 and 48 h after transfection and analyzed by western blotting. Membranes were immunoblotted with a rabbit antibody to the C-terminus of LRP12/MIG13a and with mouse anti-GAPDH as a loading control.

Two *Tg(Lrp12/Mig13a-Egfp)* dams were sacrificed at E11.5, embryos were removed by laparotomy and brains were removed by dissection. After embedding in 4% low-melting point agarose, 250-μm coronal slices were prepared by vibratome sectioning (Leica VT1000S) and transferred to Nuclepore Track-Etch Membranes (Whatman) floating on culture medium as described previously (Polleux et al. 2002). Control or *Lrp12/Mig13a* SMARTpool siRNAs were injected at 10 μM along with the *pCIG-tdTomato* vector (200 ng/mL), containing the *tdTomato* reporter gene, kindly provided by Dr Roger Tsien, into the lateral ventricles of the telencephalon. One side of the lateral/dorsolateral telencephalic wall was electroporated with a BTX electroporation system (Electro Square Porator T830) with platinum electrodes (Protech International) (130 V, 2 pulses of 5 ms duration at an interval of 1 s). Slices were cultured for 2 days in vitro (DIV) prior to fixing with 4% paraformaldehyde and embedding in OCT (Optimal Cutting Temperature, Tissue-Tek OCT Compound Histomount), after which the embedded slices were resectioned at 16 μm using a cryostat (Microm Model HM 500 M Cryostat, Leica CM 3050S). Sections were immunolabeled for EGFP and counterstained with DRAQ5 to visualize cell nuclei. tdTomato was visible without antibody amplification.

We analyzed the distribution of *Lrp12/Mig13a*-positive (EGFP labeled) and siRNA transfected (tdTomato positive) cells in slices electroporated with control siRNA (from $n = 5$ embryos) or *Lrp12/Mig13* siRNA (from $n = 5$ embryos). We counted the number of transfected, tdTomato-positive cells in 2–3 fields per section (at least 100 cells per section) and calculated the ratio of transfected, tdTomato-positive cells in the lower half of the cortical wall, containing the VZ, to tdTomato-positive cells in the upper half, containing the preplate. The Student's *t*-test was performed on the 2 sets of data with Microsoft Excel.

Results

Lrp12/Mig13a Is Expressed in Preplate Neurons Destined for the Subplate

We identified murine and human homologs of *mig-13* by tBLAST search of human and mouse genome sequences using the protein sequence of *C. elegans mig-13* as a query. *Mus musculus* LRP12/MIG13A is a novel transmembrane domain containing glycoprotein with maximal expression levels during embryonic CNS development (data not shown). The translated sequence for *Mus musculus* LRP12/MIG13A (Genbank accession number NM 172814) has 92% overall identity to *Homo sapiens* LRP12/MIG13A. To map the expression of *Lrp12/Mig13a* on a cellular level, we generated lines of bacterial artificial chromosome transgenic mice that express the *Egfp* reporter gene under the control of the native *Lrp12/Mig13a* locus [*Tg(Lrp12/Mig13a-Egfp)*] (Gong et al. 2003). At the preplate stage, immunostaining coronal sections of E12.5 *Tg(Lrp12/Mig13a-Egfp)* mouse telencephalon with anti-LRP12/MIG13A and anti-EGFP antibodies revealed a zone of double-labeled cells in the superficial layer of the dorsal telencephalon (Fig. 1*a*,*b*). In the E12.5 telencephalic wall, *Lrp12/Mig13a* messenger RNA also localizes to a superficial cortical layer close to the pial surface (Supplementary Fig. 1).

In the mouse, cumulative labeling with the thymidine analog BrdU has shown that the first neuronal progenitors exit the cell cycle in the rostrolateral aspect of the dorsal telencephalic VZ. Neurons produced at the onset of neurogenesis, E10.5–E11.5 in the mouse, form the preplate layer. To correlate the timing of the penultimate cell division and expression of *Lrp12/Mig13a*, we injected pregnant *Tg(Lrp12/Mig13a-Egfp)* dams with BrdU between E10.5 and E12.5 and assayed BrdU accumulation in *Lrp12/Mig13a*-positive cells during early phases of cortical development. At E13.5, the vast majority of EGFP/BrdU double-labeled cells were observed in embryos exposed to BrdU on E10.5 or E11.5, suggesting that *Lrp12/Mig13a*-positive cells undergo terminal divisions between E10.5 and E11.5 (Fig. 2*a*,*b*). BrdU labeling a day later (E12.5) allowed us to trace the position of preplate-derived *Lrp12/Mig13a*-positive cells relative to later-born neurons, which form the cortical plate. At E14.5, the preplate has split into the superficial marginal zone and the deeper subplate. Very few double-labeled (BrdU/*Lrp12/Mig13a*) cells were observed in lateral neocortical areas of E14.5 embryos exposed to BrdU on E12.5, when cells destined for the cortical plate undergo terminal cell division (Fig. 2*a*,*b*). While the majority of cells born on E12.5 were located in the cortical plate, BrdU-positive cells were seen positioned beneath the cortical plate, among migrating neurons and subplate neurons. In E11.5 embryos, *Lrp12/Mig13a*-positive cells coexpressed TUJ1 by immunocytochemistry, which identified them as postmitotic neurons. *Lrp12/Mig13a*/TUJ1-positive neurons were located above the cortical VZ, in the superficial layer of the E11.5 telencephalic wall (Fig. 2*c*,*d*). These experiments show that *Lrp12/Mig13a* expression is restricted to preplate neurons.

We examined whether *Lrp12/Mig13a*-positive preplate neurons included precursors of Cajal–Retzius neurons within the marginal zone that express the markers RELN and Calretinin (CALB2) or interneurons that express the marker Calbindin (CALB1) (Meyer and Goffinet 1998; Hevner et al.

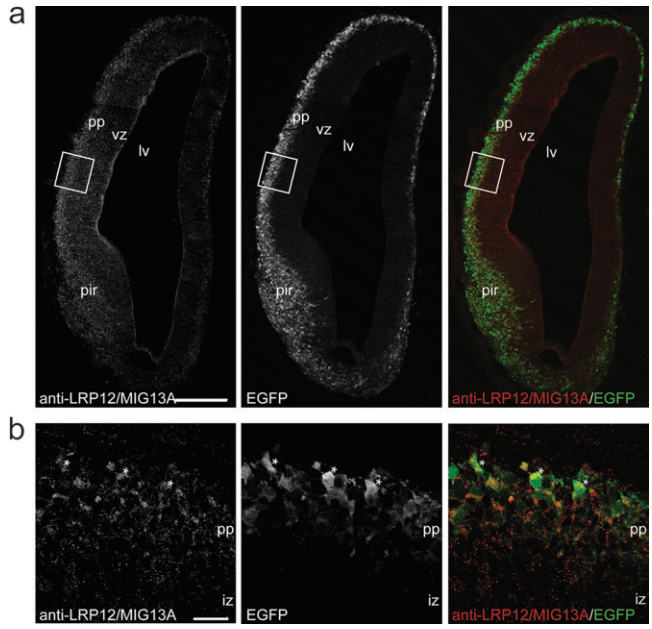

Figure 1. Expression of *Lrp12/Mig13a* in the preplate layer of embryonic *Tg(Lrp12/Mig13a-Egfp)* mouse brain. (*a*) LRP12/MIG13A and EGFP are coexpressed in the same brain regions. Twenty micrometer coronal cryosections of E12.5 *Tg(Lrp12/Mig13a-Egfp)* mouse brain were immunostained with anti-LRP12/MIG13A and anti-EGFP antibodies. Composites of confocal *z*-stacks are shown. Scale bar, 200 μm. (*b*) High-power pictures of the preplate in the areas boxed in (*a*) to show colocalization of LRP12/MIG13A and EGFP in single cells, some of which are highlighted by a star. Single optical confocal sections are shown. Scale bar, 20 μm. iz, Intermediate zone; lv, lateral ventricle; pir, piriform cortex; pp, preplate; vz, ventricular zone.

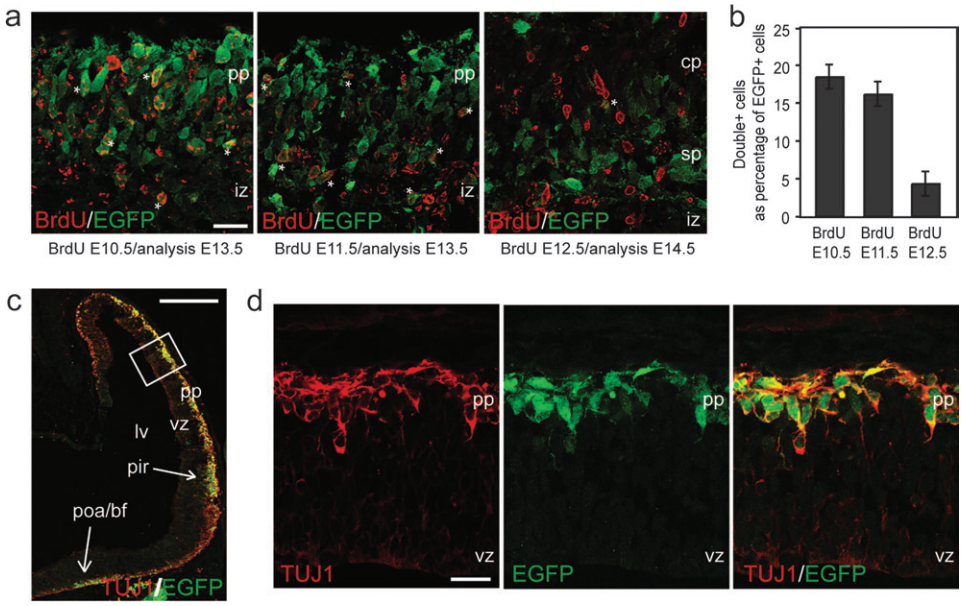

Figure 2. *Lrp12/Mig13a* is expressed in cortical neurons generated between E10.5 and E11.5. (*a*) BrdU birthdating of *Lrp12/Mig13a*-positive cells in the developing telencephalic wall. Pregnant *Tg(Lrp12/Mig13a-Egfp)* females were injected with BrdU at E10.5, E11.5, and E12.5, and embryos were analyzed at E13.5 or E14.5 as indicated. Twenty micrometer coronal sections in the anterior forebrain at the level of the anterior commissure of *Tg(Lrp12/Mig13a-Egfp)* mouse embryos were immunostained for BrdU and EGFP. Some BrdU and EGFP double-positive cells are labeled with stars. Confocal single optical sections are shown. Scale bar, 20 μm. (*b*) Quantitation of BrdU birthdating in (*a*). BrdU-positive, EGFP-positive, and BrdU-EGFP-double-positive cells were counted in lateral areas of the cerebral cortex in coronal sections of the indicated experimental conditions. Mean values and standard error for double-positive cells were calculated from an average of 800 counted cells from 2 independent experiments for each condition. (*c*, *d*) *Lrp12/Mig13a* is expressed in early generated TUJ1-positive neuronal cells in the telencephalic wall. Twenty micrometer coronal sections of an E11.5 *Tg(Lrp12/Mig13a-Egfp)* mouse embryo were immunostained for EGFP and TUJ1. Boxed areas in (*c*) are magnified in (*d*). A confocal *z*-stack is shown in (*c*) and a confocal single optical section in (*d*). Scale bars, 200 μm in (*c*) and 20 μm in (*d*). bf, Basal forebrain; cp, cortical plate; iz, intermediate zone; lv, lateral ventricle; pir, piriform cortex; poa, preoptic area; pp, preplate; sp subplate; vz, ventricular zone.

2003). At E13.5, *Lrp12/Mig13a*-expressing cells did not coexpress CALB1, RELN, or CALB2 (Supplementary Fig. 2). RELN-positive Cajal–Retzius cells were superficial to *Lrp12/Mig13a-EGFP*-positive neurons (Supplementary Fig. 2). *Lrp12/Mig13a*-positive cells were also distinct from the TAG-1-positive plexiform layer in the intermediate zone (Fig. 3*a*,*b*). *Lrp12/Mig13a*-EGFP-positive preplate neurons coexpressed the microtubule-associated protein MAP2, a marker for mouse preplate neurons that segregate both to the marginal zone and to the subplate (Crandall et al. 1986; Chun et al. 1987). The coexpression of MAP2 by *Lrp12/Mig13a*-positive cells in the newly formed subplate at E14.5 (Fig. 3*c*) showed that *Lrp12/Mig13a* marks a subpopulation of preplate neurons that later reside in the subplate. *Lrp12/Mig13a* expression in the subplate layer persisted through E18 (Fig. 3*d*,*e*) and declined in the early postnatal period (data not shown). Thus, *Lrp12/Mig13a*-positive neurons constitute a subpopulation of preplate neurons that segregate into the subplate during early cortical development.

Neurons Expressing Lrp12/Mig13a Pioneer Commissural Axon Projections

During corticogenesis, transient neuronal populations of the preplate and subplate extend descending axons to subcortical targets and corticocortical axons to targets in the ipsilateral or contralateral hemisphere. The latter pioneer axon tracts that project through the anterior commissure. At E13.5, *Lrp12/Mig13a*-positive preplate neurons extended axons that descended into the intermediate zone before navigating through the subpallium and exiting the cortical hemisphere via the anterior commissure (Fig. 4*a*,*b* and Supplementary Fig. 3*a*). In contrast, thalamocortical fibers immunopositive for anti-CALB2 (Del Rio et al. 2000) projected to the internal capsule (Fig. 4*a*,*b*,*d*); *Lrp12/Mig13a*-positive fibers were not detected in this pathway. *Lrp12/Mig13a*-positive fibers did not coexpress the transient axonal glycoprotein (TAG-1) (Denaxa et al. 2001), a marker for corticothalamic projections at the preplate stage (Fig. 4*a*,*c*). TAG-1-positive fibers extended through the upper aspect of the intermediate zone, above *Lrp12/Mig13a*-positive fibers (Fig. 4*c*). *Lrp12/Mig13a*-positive axons were immunopositive for antibodies against the cell adhesion molecule L1, a marker for commissural projections (Fukuda et al. 1997; Jones et al. 2002; Morante-Oria et al. 2003) (Supplementary Fig. 3*b*). These results show that *Lrp12/Mig13a* is expressed in a subpopulation of preplate neurons, whose axons pioneer projections to the contralateral hemisphere via the anterior commissure. At later stages, this projection forms corticocortical connections with the contralateral temporal lobe.

Although studies on the development of cortical malformations, including those in *reeler* mice, have defined the principal steps of corticogenesis, the dynamics of cell movements in the preplate zone have not been examined. To examine tangential movements of preplate neurons (Tomioka et al. 2000), we prepared coronal slices of E12.5 *Tg(Lrp12/Mig13a-Egfp)* mouse forebrain and used multiphoton microscopy to acquire time-lapse images of living *Lrp12/Mig13a*-positive preplate cells. Approximately 5% of *Lrp12/Mig13a*-expressing cells migrated along a ventral tangential trajectory in the middle of the preplate layer and at the boundary of the preplate and VZ during the period we imaged (Fig. 5*a*,*b*, Supplementary Movie

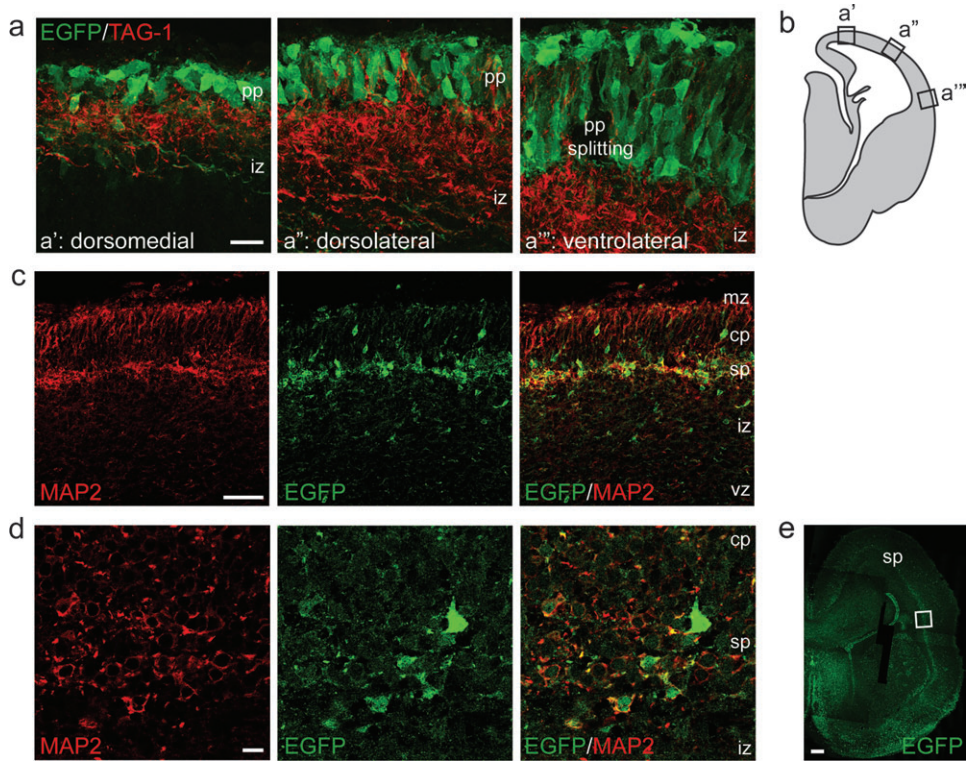

Figure 3. *Lrp12/Mig13a* expression identifies a subpopulation of preplate neurons destined for the subplate layer. (*a*) *Lrp12/Mig13a* expression does not overlap with TAG-1 immunostaining in the E13.5 cerebral cortex. Twenty micrometer coronal cryosection was immunostained for TAG-1 and EGFP and dorsomedial (*a'*), dorsolateral (*a''*), and ventrolateral (*a'''*) areas are shown as indicated in (*b*). Scale bar, 10 μm. (*c*) *Lrp12/Mig13a* expression overlaps with MAP2 in the subplate. Twenty micrometer coronal section of an E14.5 *Tg(Lrp12/Mig13a-Egfp)* mouse embryo was immunostained for EGFP and MAP2, and a lateral area of the developing cerebral cortex is shown. Scale bar, 100 μm. (*d*) A subset of MAP2-positive subplate cells also expresses *Lrp12/Mig13a* at E18.5. Twenty micrometer coronal section of an E18.5 *Tg(Lrp12/Mig13a-Egfp)* mouse embryo was immunostained for EGFP and MAP2, and a lateral area of the developing cerebral cortex is shown as indicated in (*e*). Scale bar, 10 μm. (*e*) Twenty micrometer coronal sections of an E18.5 *Tg(Lrp12/Mig13a-Egfp)* mouse embryo were immunostained for EGFP, and a lateral area of the developing cerebral cortex is boxed to indicate the position of the images in (*d*). Scale bar, 200 μm. All images are confocal single optical sections except in (*e*) a composite of confocal *z*-stacks confocal *z*-stacks is shown. cp, cortical plate; iz, intermediate zone; mz, marginal zone; pp, preplate; sp subplate, vz, ventricular zone.

1). *Lrp12/Mig13a*-expressing cells were not observed in the superficial subpial aspect of the preplate zone, where Cajal–Retzius cell migration has been reported. During periods of movement, *Lrp12/Mig13a*-positive, EGFP-labeled neurons polarized and extended and retracted a broad lamellipodium (Fig. 5*a,b*, Supplementary Movie 1) while migrating at speeds ranging from 0 to 140 μm/h (average velocity, 18 μm/h) (Supplementary Fig. 4*a,b*). These findings reveal the dynamics of tangential migrations within the preplate layer prior to cortical plate formation.

Lrp12/Mig13a Functions in Neuronal Migrations during Cortical Development

To determine whether *Lrp12/Mig13a* functions in cell motility during the preplate to cortical plate transition, we used SMARTpool siRNAs to knockdown *Lrp12/Mig13a* levels. Cotransfection of a full-length *Lrp12/Mig13a* cDNA and SMARTpool *Lrp12/Mig13a* siRNAs into HEK 293T cells resulted in complete knock down of LRP12/MIG13A protein levels within 24 h, suggesting efficient posttranscriptional silencing of *Lrp12/Mig13a* (Supplementary Fig. 5). To examine the effect of silencing *Lrp12/Mig13a* expression in developing murine neocortex, coronal slices of E11.5 *Tg(Lrp12/Mig13a-Egfp)* mouse forebrain were coelectroporated with either control or *Lrp12/Mig13a* SMARTpool siRNAs and tdTomato as an indicator for electroporated cells. After 2 DIV, the position of cells expressing EGFP as an indicator of endogenous *Lrp12/Mig13a* expression and the tdTomato reporter was examined by confocal microscopy. In sections of control siRNA electroporated slices, preplate formation occurred normally in both lateral and dorsolateral areas of the telencephalic wall (Supplementary Fig. 6*a,b*). After electroporation of *Lrp12/Mig13a* SMARTpool siRNAs, 2 classes of defects in cell migration were observed. First, *Lrp12/Mig13a*-positive, EGFP labeled cells that expressed tdTomato were located in the deep layers of the neocortex, suggesting a failure to migrate into the preplate zone. Second, cells that expressed only tdTomato also accumulated in the deep layers of the telencephalic wall, suggesting nonautonomous defects in radial migrations (Supplementary Fig. 6*c,d*). Thus, silencing *Lrp12/Mig13a* affects cell migrations of *Lrp12/Mig13a*-expressing cells, as well as the migrations of other cells in the developing cortex. This prompted further analysis of *Lrp12/Mig13a*-positive cells at the preplate stage of cortical development.

Movements and Changing Polarity of Preplate Neurons during Preplate Separation and Cortical Plate Formation

To examine the behavior of preplate neurons during separation of the preplate into a superficial marginal zone and deeper subplate zone, we imaged *Lrp12/Mig13a*-positive, EGFP-labeled cells in coronal forebrain slices of E13.5 *Tg(Lrp12/Mig13a-Egfp)* mice. Real-time imaging by multiphoton

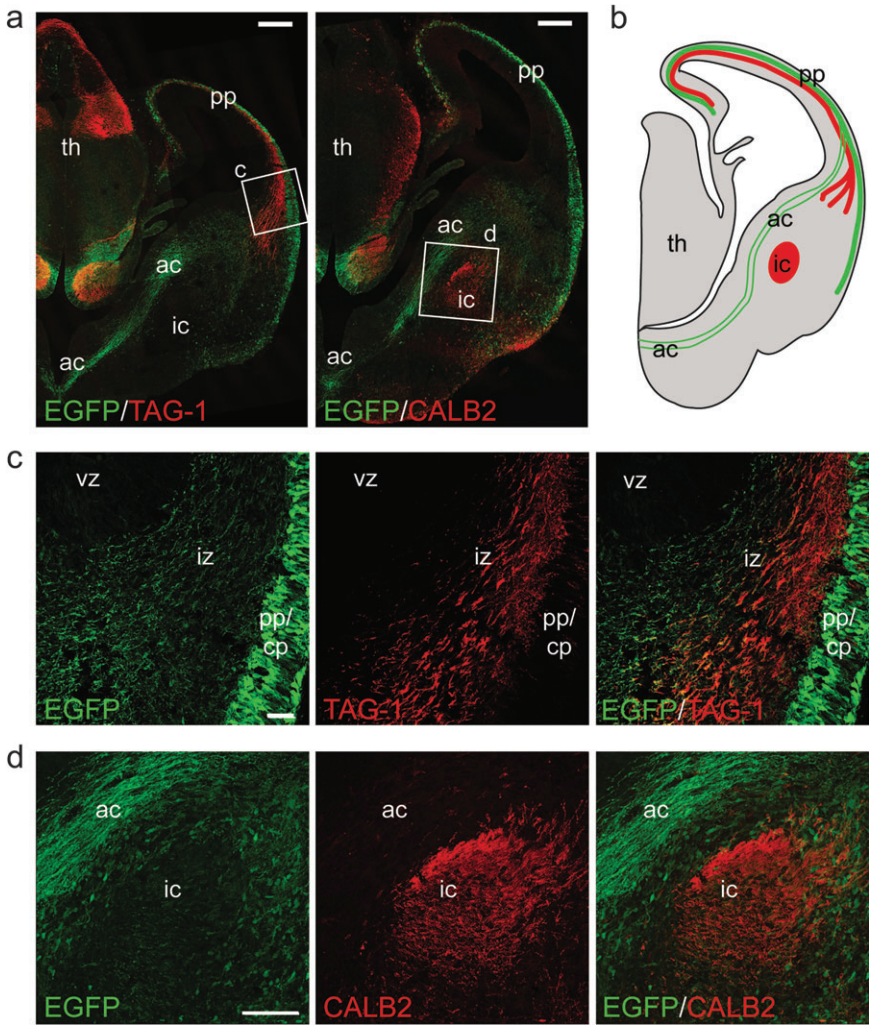

Figure 4. *Lrp12/Mig13a*-expressing preplate neurons pioneer anterior commissural projections. (*a*) Twenty micrometer coronal cryosections were immunostained for EGFP/TAG-1 and EGFP/CALB2. In the subpallium, *Lrp12/Mig13a* expression is found in axonal tracts leading exclusively to the anterior commissure. TAG-1-positive fibers do not project to the anterior commissure but temporarily terminate in the subpallium before later reaching the thalamus. Anti-CALB2 antibodies labeled thalamocortical fibers in the internal capsule, which is devoid of *Lrp12/Mig13a* expression. Scale bars, 200 μm. High magnifications of boxed areas are shown in (*c*) and (*d*). (*b*) Drawing of an E13.5 coronal brain section summarizing the distinct *Lrp12/Mig13a*-positive (green) and TAG-1-positive (red) corticofugal projections, as well as the CALB2-positive (red) thalamocortical fibers in the internal capsule. (*c*) High magnification of the area of the lateral preplate and intermediate zone immunostained for EGFP/TAG-1 in (*a*) showing that the *Lrp12/Mig13a*-positive fibers in the intermediate zone of the telencephalic wall are largely distinct from TAG-1-positive fibers. Scale bar, 20 μm. (*d*) High magnification of the area of the internal capsule immunostained for EGFP/CALB2 in (*a*). *Lrp12/Mig13a*-positive fibers are traveling in a bundle leading to the anterior commissure, but no *Lrp12/Mig13a* expression is detected in the internal capsule, which is immunolabeled by anti-CALB2 antibodies. Scale bar, 20 μm. Composites of confocal z-stacks are shown in (*a*) and single optical confocal sections are shown in (*c*) and (*d*). ac, Anterior commissure; cp, cortical plate; ic, internal capsule; iz, intermediate zone; pp, preplate; th, thalamus; vz, ventricular zone.

microscopy revealed dynamic changes in the polarity and motility of *Lrp12/Mig13a*-positive cells (Fig. 6*a*,*b*). *Lrp12/Mig13a*-positive cells assumed an elongated morphology and aligned along the radius of the cortical wall. In live images, during preplate separation, *Lrp12/Mig13a*-positive cells drifted into the deeper subplate position (Fig. 6*a*,*b*). Thus, as the subplate formed, *Mig13a/Lrp12*-positive cells moved into the emerging subplate layer.

The changing orientation of preplate neurons at late stages of preplate development followed a spatiotemporal gradient. In dorsal aspects of E12.5–E13.5 telencephalon, *Lrp12/Mig13a*-positive preplate neurons assumed an apparently random orientation (Fig. 6*c*). At the onset of cortical plate formation in the ventrolateral telencephalic wall (E13.5), *Lrp12/Mig13a*-positive preplate neurons polarized toward the pial surface in a pseudocolumnar pattern (Fig. 6*d*). These radially oriented cells were intercalated with *Lrp12/Mig13a*-negative cells and some extended neurites into the intermediate zone (stars in Fig. 6*d*).

To determine the polarity of *Lrp12/Mig13a*-positive neurons during preplate separation, we immunolabeled cells for the cis-Golgi matrix protein GM130 (Nakamura et al. 1995) in conjunction with the nuclear marker DAPI. To measure the orientation of the Golgi apparatus relative to the neuronal soma, we drew a line from the center of the nucleus to the GM130-immunopositive Golgi apparatus and mapped the orientation of the line relative to the radius of the cortical wall (Fig. 7*e*). At E12.5, the position of the Golgi apparatus of *Lrp12/Mig13a*-positive cells was oriented largely parallel to the pial surface (Fig. 7*a*,*d*). During the initial stage of preplate separation at E13.5, the majority of *Lrp12/Mig13a*-positive cells were radially aligned, with their Golgi apparatus

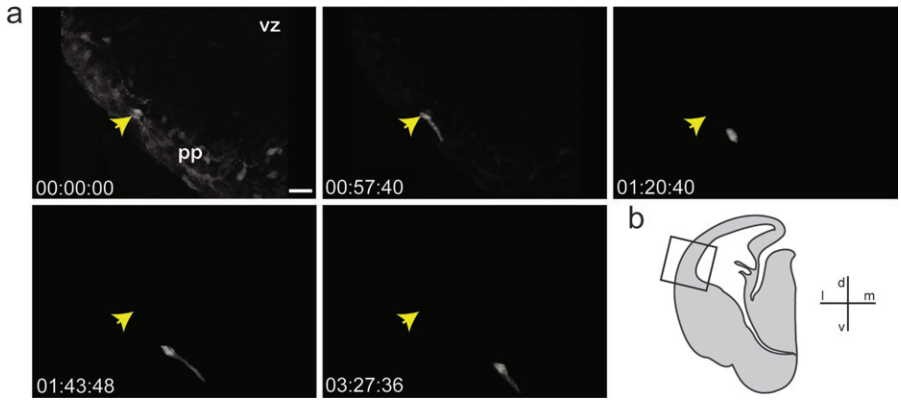

Figure 5. A subset of *Lrp12/Mig13a*-positive preplate cells migrates ventrally tangentially. (*a*) An acute coronal forebrain slice of an E12.5 *Tg(Lrp12/Mig13a-Egfp)* embryo was imaged for EGFP by multiphoton microscopy over a time period of 4 h. Still frames at the indicated time points show the migration of an *Lrp12/Mig13a*-positive cell. The starting point is highlighted with a yellow arrow in the first and all following frames. After the first frame, the *Lrp12/Mig13a*-positive preplate cell is isolated and the background is faded out. All images are maximum intensity projections of the acquired *z*-stacks. Scale bar, 20 μm. Orientation: dorsal to the top left and lateral to the bottom left. (*b*) Schematic drawing of an E12.5 coronal forebrain section with a rectangular box in the lateral developing neocortex indicating the imaged area. d, dorsal; l, lateral; m, medial; pp, preplate; v, ventral; vz, ventricular zone.

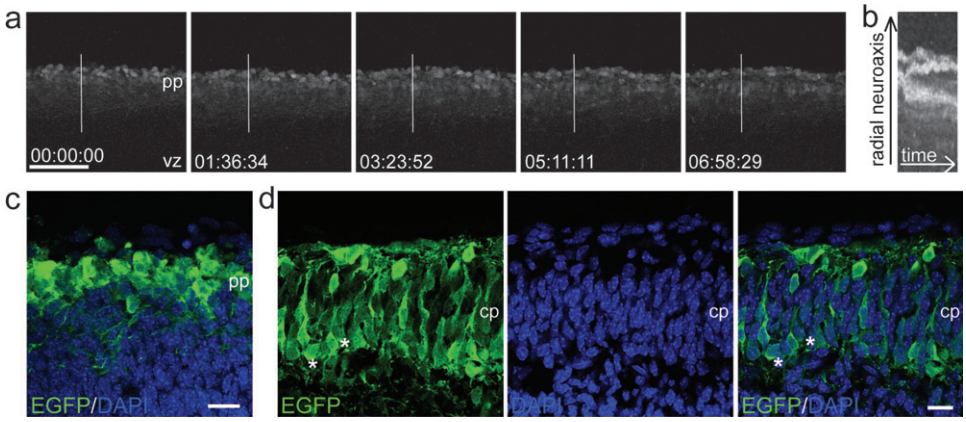

Figure 6. Changes in the orientation and alignment of *Lrp12/Mig13a*-expressing neurons during preplate separation. (*a*) Acute coronal slice of an E13.5 forebrain of a *Tg(Lrp12/Mig13a-Egfp)* mouse was imaged live for EGFP by multiphoton microscopy over 7 h. Still frames at the indicated time points show *Lrp12/Mig13a*-positive preplate cells acquiring a radial orientation and segregating into presumptive subplate populations. The white line indicates the position of the kymogram in (*b*). Scale bar, 100 μm. (*b*) Graphical representation of the position of *Lrp12/Mig13a*-positive neurons over time of development. The radial neuroaxis is plotted against the time. A subset of *Lrp12/Mig13a*-positive cells moves away from the pial surface. (*c*) Twenty micrometer coronal cryosection of a dorsal area of E13.5 forebrain of a *Tg(Lrp12/Mig13a-Egfp)* mouse was immunostained for EGFP and DAPI. The preplate has not yet separated and multiple *Lrp12/Mig13a*-positive cells are forming projections. (*d*) Twenty micrometer coronal cryosections of a lateral area of E13.5 forebrain of a *Tg(Lrp12/Mig13a-Egfp)* mouse, where the preplate is separating and the cortical plate develops, were immunostained for EGFP and stained for DAPI. *Lrp12/Mig13a*-expressing cells are radially oriented, extend a thick process toward the pial surface and some also continue to form a projection toward ventral areas (marked by stars). *Lrp12/Mig13a*-positive future subplate cells are transiently integrated in the developing cortical plate and radially intercalate with *Lrp12/Mig13a*-negative cells. Scale bars for (*c*) and (*d*) 20 μm. cp, cortical plate; pp, preplate.

positioned between the nucleus and the pial membrane (Fig. 7*b*,*d*) and a process extended toward the pia. These cells appeared to intercalate with the arriving cortical plate neurons, which were also radially aligned (Pinto-Lord et al. 1982). These data reveal for the first time a dynamic regulation of the polarity of future subplate neurons during preplate separation (Fig. 7*f*).

Lrp12/Mig13a-Positive Preplate Neurons Fail to Undergo Changes in Cell Polarity in Developing Reeler Neocortex

Subsequent to the appearance of the cortical plate, after E13 in mouse, cohorts of cells migrate through the intermediate zone and emerging subplate to the boundary of the cortical plate and marginal zone, where they form a series of neuronal layers. In the *reeler* mouse, however, later-generated neurons fail to migrate through the emerging subplate, leaving the preplate population as an intact "superplate." Although cohorts of cells formed at the same time in the 2 genotypes give rise to the same classes of neurons, neurons are improperly oriented and the neuronal layers are inverted in the *reeler* mutant mouse (Caviness 1982; Goffinet 1984; Tissir and Goffinet 2003). These studies suggested a model in which the cortical malformation seen in *reeler* mice results from a failure of cortical plate formation. This failure has been attributed to defects in the cessation of the migration of later-generated neurons destined for the cortical plate (Caviness 1982; Goffinet 1984). To examine whether cell movements at an earlier phase, prior to cortical plate formation, were defective in *reeler* mice, we crossed transgenic *Tg(Lrp12/Mig13a-Egfp)* mice with mice lacking Reelin. *Tg(Lrp12/Mig13a-Egfp)* embryos with the *reeler* (*rl/rl*) mutation (*B6C3Fea-Tg(Lrp12/Mig13a-Egfp)* a*Reln*^{rl}/a*Reln*^{rl}) were identified by PCR (D'Arcangelo et al.

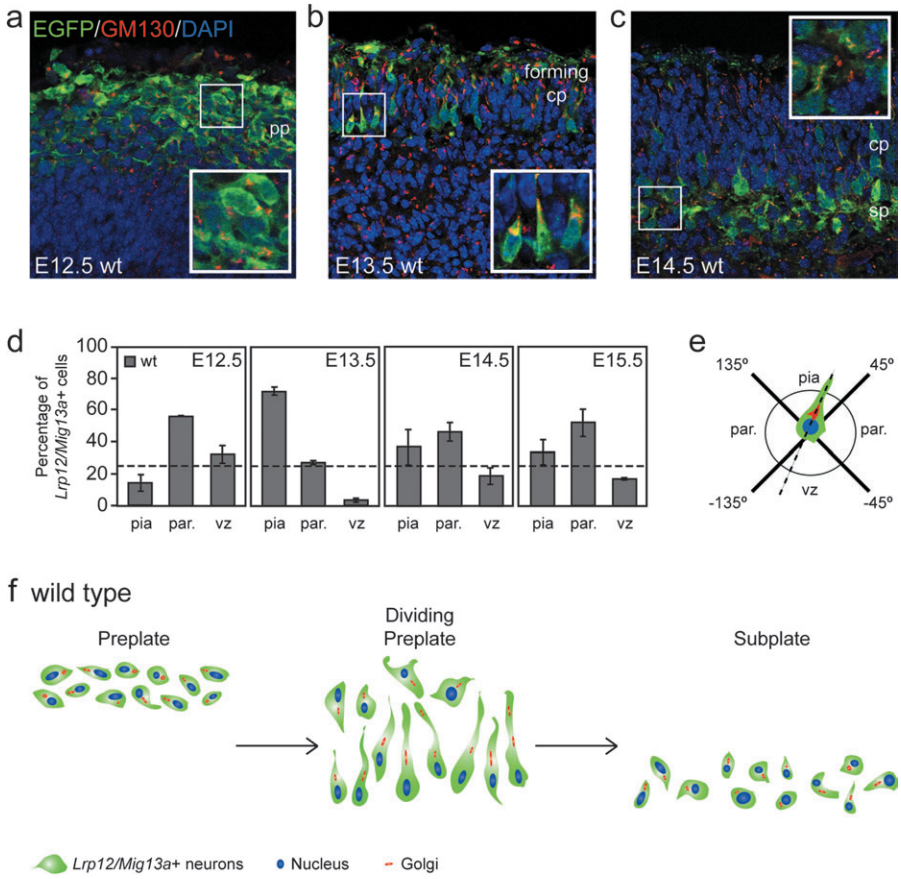

Figure 7. The changes in *Lrp12/Mig13a*-positive preplate cell polarity during preplate separation and cortical plate formation. (*a–c*) Twenty micrometer coronal cryosections of *Tg(Lrp12/Mig13a-Egfp)* mice of the indicated ages were immunostained for EGFP and GM130 and counterstained for DAPI. During this developmental series, *Lrp12/Mig13a*-positive wild-type (wt) cells change morphology and orientation. Boxed areas are shown at higher magnification in the insets to highlight examples of preplate cell polarity. (*d*) Quantitative analysis of preplate cell orientation from E12.5 to E15.5 in wt mice. The orientation of *Lrp12/Mig13a*-positive preplate cells was scored and grouped into bins according to the schematic drawing in (*e*). The horizontal dashed line indicates expected distribution for random orientation (25%); the parallel bar indicates the sum of the 2 parallel quarters. *Lrp12/Mig13a*-positive cell orientation was statistically significantly different from random distribution (25%) at E12.5 ($P < 0.05$), at E13.5 ($P < 0.001$), and at E14.5 ($P < 0.05$) but not at E15.5 (χ^2 test). A total of at least 200 cells per age out of 2 independent experiments were scored. (*e*) Schematic drawing of the assigned bins for scoring preplate cell orientation. (*f*) Model of preplate cell orientation during preplate separation and mechanism of preplate separation. During initial stages of preplate separation (E13), *Lrp12/Mig13a*-positive neurons acquire a bipolar morphology with the Golgi apparatus oriented toward the pial surface. The alignment of *Lrp12/Mig13a*-positive preplate neurons with the radial axis results in the formation of a transient columnar arrangement of *Lrp12/Mig13a*-expressing neurons during the segregation of preplate neurons into a superficial marginal zone and an underlying subplate. The transient polarization of *Lrp12/Mig13a*-positive preplate neurons might facilitate radially migrating cortical plate neurons to move through the emerging subplate zone into the nascent cortical plate. *Lrp12/Mig13a*-positive cells are shown in green with nuclei colored in blue and Golgi in red. All images are confocal single optical sections. cp, cortical plate; par, parallel to pial surface; pia, pial surface; pp, preplate; sp, subplate; vz, ventricular zone.

1996; Gong et al. 2003; Jossin and Goffinet 2007). We examined embryos between the ages of E12.5–15.5 and measured the distance of *Lrp12/Mig13a*-positive preplate neurons from the pial surface, comparing their distribution in *rl/rl* and wild-type littermates (Supplementary Fig. 7*a–d*). In wild-type cortex, *Lrp12/Mig13a*-positive cells progressively moved from subpial locations at E12.5 to deeper regions of cortex at E15.5, while in *rl/rl* cortex *Lrp12/Mig13a*-positive cells remained in subpial positions throughout the time periods examined, confirming that they did not form a subplate layer.

We next examined the dynamics of polarity of *Lrp12/Mig13a*-positive preplate neurons in *rl/rl* embryonic cortex. Temporal changes in the morphology and orientation of *Lrp12/Mig13a*-positive neurons were measured by determining the orientation of the Golgi apparatus relative to the radius of the cortical wall (Fig. 8*e*). At E12.5, a stage prior to preplate splitting, the shape and orientation of *Lrp12/Mig13a*-positive preplate neurons in *rl/rl* mutant mouse neocortex (Fig. 8*a,d*) were indistinguishable from their counterparts in wild-type neocortex (Figs 7*a,d* and 8*d*). However, at E13.5, just before the preplate splits, *Lrp12/Mig13a*-positive neurons in the *rl/rl* neocortex failed to adopt a bipolar shape and align with the radial axis (Fig. 8*b,d*) like their counterparts in wild-type neocortex. At E14.5, after the segregation of preplate neurons in the wild-type neocortex, small but significant differences were seen in the morphology and orientation of *Lrp12/Mig13a*-positive cells in the mutant superplate (Fig. 8*c,d*) and the wild-type subplate (Figs 7*c,d* and 8*d*). After the segregation of preplate neurons in the wild-type neocortex at E15.5, *Lrp12/Mig13a*-positive cells were randomly oriented both in the wild-type subplate and in the *rl/rl* superplate. These studies identify the earliest known defect in *reeler* cortical patterning and demonstrate that *Lrp12/Mig13a*-positive *reeler* preplate cells do not undergo temporal changes in neuronal morphology and orientation during early stages of corticogenesis.

Since genetic and pharmacological experiments have shown that inhibitors of SFKs generate a *reeler*-like cortical malformation (Hanke et al. 1996; Arnaud et al. 2003; Bock and Herz 2003;

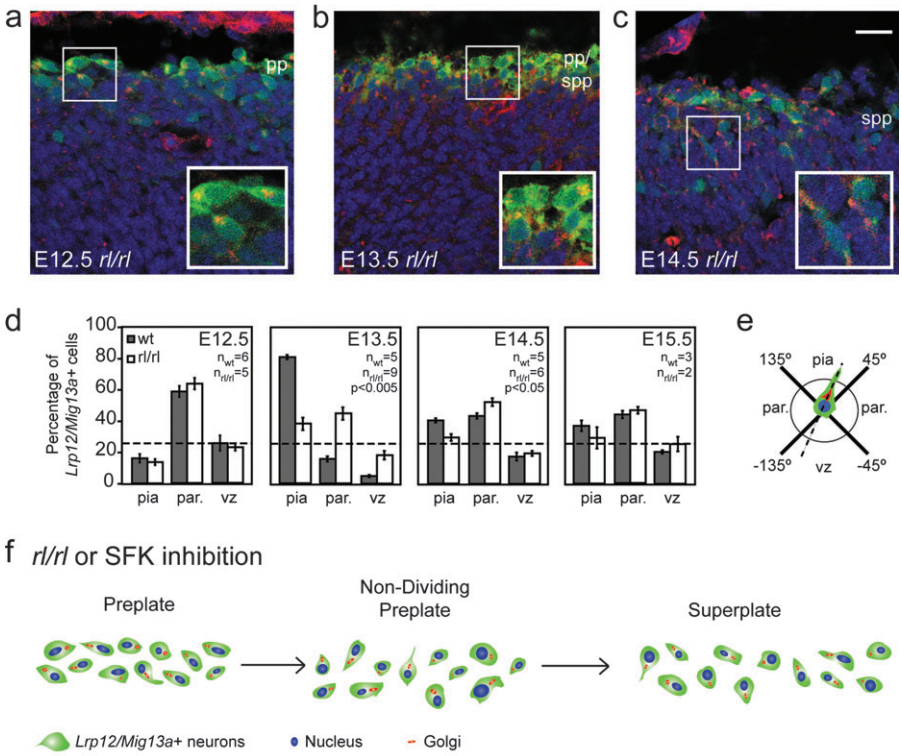

Figure 8. The changes in *Lrp12/Mig13a*-positive preplate cell polarity during preplate separation and cortical plate formation do not occur in *reeler* mutant mice. (*a–c*) Twenty micrometer coronal cryosections of *Tg(Lrp12/Mig13a-Egfp)* mice, which are homozygous for the *reeler* mutation *(rl/rl)*, of the indicated ages were immunostained for EGFP and GM130 and counterstained for DAPI. During this developmental series, *Lrp12/Mig13a*-positive *rl/rl* cells no not appear to undergo significant cell shape and orientation changes as observed in wild-type (wt) littermates. Boxed areas are shown at higher magnification in the insets to highlight examples of preplate cell polarity. In addition, *Lrp12/Mig13a*-positive *rl/rl* cells do not segregate into the subplate but remain underneath the pia forming the superplate (*b*, *c*). (*d*) Quantitative analysis of preplate cell orientation from E12.5 to E15.5 in wt and *rl/rl* mice. The orientation of *Lrp12/Mig13a*-positive preplate cells was scored and grouped into bins according to the schematic drawing in (*e*). The horizontal dashed line indicates expected distribution for random orientation (25%); the parallel bar indicates the sum of the 2 parallel quarters. *Lrp12/Mig13a*-positive cell orientation was statistically significantly different from random distribution (25%) for wt ($P < 0.001$) and *rl/rl* ($P < 0.001$) at E12.5, for wt ($P < 0.001$) and *rl/rl* ($P < 0.005$) at E13.5, and for wt ($P < 0.005$) at E14.5 (χ^2 test). The number of brains analyzed per genotype (n_{wt}, $n_{rl/rl}$) and age are indicated in each panel, and 90–350 cells per brain were scored. The statistically significant difference between wt and *rl/rl Lrp12/Mig13a*-positive cells was determined (*t*-test) at each age and indicated as *P* value in the panels if applicable. (*e*) Schematic drawing of the assigned bins for scoring preplate cell orientation. (*f*) Model of preplate cell orientation during preplate separation in the *rl/rl* mutant. The transient polarization of *Lrp12/Mig13a*-positive preplate neurons observed in the wt situation does not occur in *reeler* cortex or in cortical slices treated with the SFK inhibitor PP2. Subsequently, the preplate does not separate and the *Lrp12/Mig13a*-positive cells remain in the superplate. *Lrp12/Mig13a*-positive cells are shown in green with nuclei colored in blue and Golgi in red. Scale bars for (*a–c*), 20 μm. All images are confocal single optical sections. cp, Cortical plate; par, parallel to pial surface; pia, pial surface; pp, preplate; SFK; spp, superplate; vz, ventricular zone.

Jossin et al. 2003), we examined the effect of the SFK inhibitor PP2 on temporal changes in polarity of *Lrp12/Mig13a*-positive preplate neurons in developing *Tg(Lrp12/Mig13a-Egfp)* neocortex. When coronal slices of E12.5 *Tg(Lrp12/Mig13a-Egfp)* mouse forebrain were treated with PP2 for 2 DIV, the temporal changes in *Lrp12/Mig13a*-positive cell shape and polarity seen in control slice cultures did not occur (Supplementary Fig. 8). In addition, in PP2-treated slices, the preplate did not separate (Supplementary Figs 7*e–g* and 8*c*) and *Lrp12/Mig13a*-positive cells were randomly oriented (Supplementary Fig. 8*c,d*). These findings suggest that the neuropathological changes that occur in *reeler* or in mice lacking SFKs might result from a failure of preplate neurons to polarize toward the pial surface during the stage when preplate neurons segregate into the marginal zone and subplate layer (Fig. 8*f*).

Discussion

These experiments demonstrate that preplate neurons that express *Lrp12/Mig13a* form specific axon projections and undergo previously unrecognized Reln-dependent changes in cell polarity just prior to cortical plate formation in developing neocortex. During early and mid-preplate stages, *Lrp12/Mig13a*-positive neurons extended pioneering axons that project to the contralateral hemisphere. Live imaging of *Lrp12/Mig13a*-positive, EGFP-labeled neurons in the early preplate revealed that preplate neurons migrated tangentially in the preplate layer. The mode of neuronal movement during these tangential migrations involved the rapid extension and retraction of a broad lamellipodial process. After E13.5, as the cortical plate emerged in the lateral telencephalic wall, these tangential movements paused as *Lrp12/Mig13a*-positive neurons polarized toward the pial surface. Subsequently, preplate neurons moved into positions above (marginal zone) or below (subplate) the cortical plate, with *Lrp12/Mig13a*-positive neurons drifting into the lower subplate region. In *reeler* mutant mice, this transient change in neuronal polarity did not occur and the preplate failed to separate. A similar defect in neuronal polarity occurred in *Tg(Lrp12/Mig13a-Egfp)* neocortex treated with PP2, an inhibitor of SFKs (Hanke et al. 1996). Taken together, these experiments reveal an earlier defect in *reeler* corticogenesis than previously realized and

suggest that Reln-signaling-dependent changes in cell polarity are involved in the formation of a pseudolayer just prior to assembly of the cortical plate.

Preplate neurons that express the evolutionarily conserved gene *Lrp12/Mig13a* represent a subpopulation of future subplate neurons that establish connections with the contralateral hemisphere. These data highlight the little-appreciated heterogeneous nature of preplate and subplate neuron populations and provide a novel genetic marker to positively distinguish neurons pioneering projections to the anterior commissure from those pioneering projections toward the thalamus.

The alignment of *Lrp12/Mig13a*-positive preplate neurons with the radial axis resulted in the formation of a transient columnar arrangement during the segregation of preplate neurons into a superficial marginal zone and an underlying subplate. To our knowledge, this is the first description of the morphology of neurons destined for the subplate during cortical plate formation, and our observations suggest that these active changes in preplate/subplate neuron morphology and orientation might be required for the cortical plate neurons to efficiently migrate past subplate neurons to their final destination beneath the marginal zone. These results also suggest a potential role for neuron–glia interaction and signaling pathways in preplate cell polarity as radial alignment of neurons is largely dependent on their interactions with radial glia in the developing cortex (Rakic 1972).

Transient polarization of *Lrp12/Mig13a*-positive preplate neurons did not occur in *reeler* cortex or in cortical slices treated with the SFK inhibitor PP2. This lack of preplate neuron polarization was associated with a failure of preplate splitting. The failure of preplate neurons to polarize in the absence of RELN or SFK signaling could be a consequence of the defects in radial glial morphology previously described in *reeler*[48] or a secondary consequence of the migratory defects observed in neurons of the *reeler* ectopic cortical plate. However, our data raise the intriguing possibility that RELN signaling between populations of preplate neurons is necessary for the observed changes in polarity and is an early patterning event required for normal cortical development.

The failure of *Lrp12/Mig13a*-positive preplate neurons to transiently polarize in the absence of RELN or SFK signaling further suggests that these pathways might converge on conserved polarity signaling pathways to control neuronal alignment and polarity during preplate splitting. Support for this idea is provided by recent studies on the role of the conserved mPar6α polarity signaling complex in the polarization and migration of neurons in the developing CNS (Arnaud et al. 2003; Shi et al. 2004; Solecki et al. 2004, 2006) and tyrosine phosphorylation of Par3 by an SFK signaling pathway during the formation of epithelia (Wang et al. 2006). Thus, SFK signaling pathways that involve conserved polarity proteins may control preplate neuron alignment into a pseudoepithelium, which we suggest may be required for proper formation of the cortical plate.

The development of the neocortex involves a series of discrete steps that include the migration of postmitotic neurons from generative zones, and the assembly of transient cell layers, which transform into a series of 6 neuronal layers. The present study reveals dynamic changes in preplate neuron movement and organization. At the preplate stage, neurons within the preplate undergo tangential migration. These migrations halt just prior to preplate separation, when preplate neurons form a columnar arrangement and *Lrp12/Mig13a*-expressing preplate cells move into the emerging subplate zone. These experiments show that *Lrp12/Mig13a*-expressing preplate cells constitute a subset of the preplate cell population that segregate into the subplate layer by an active process, which appears to involve polarity signaling pathways. We postulate that the transient polarization of *Lrp12/Mig13a*-positive preplate neurons allows radially migrating cortical plate neurons to move through the emerging subplate zone. In this model, defects in RELN signaling disrupt a sequence of preplate cell movements and changes in polarity required to coordinate the separation of the preplate and formation of the cortical plate during normal corticogenesis.

Supplementary Material

Supplementary material can be found at: http://www.cercor.oxfordjournals.org/.

Funding

National Institutes of Health grant (RO1-NS-15429-27 to M.E.H.); Deutsche Forschungsgemeinschaft to S.S.

Notes

We are grateful to Drs Cori Bargmann, Nathaniel Heintz, Hilleary Osheroff, Shiaoching Gong, and Carla Shatz for critical comments on the experiments reported and to Drs Eve-Ellen Govek and Hilleary Osheroff for reading the manuscript. We thank John Baker and Nick Didkovsky for assembling time-lapse images into a MPEG-4 movie, Drs Tom Curran, Tom Jessell, and Jacqueline Trotter for providing anti-RELN, anti-TAG-1, and anti-L1 antibodies, and Dr Roger Tsien for providing *tdTomato*. We also thank Dr Alison North and Shivaprasad Bhuvanendran in the Bio-Imaging Resource Center at the Rockefeller University for expert assistance collecting multiphoton images and Nawshin Hoque for expert technical assistance. *Conflict of Interest*: None declared.

References

Allendoerfer KL, Shatz CJ. 1994. The subplate, a transient neocortical structure: its role in the development of connections between thalamus and cortex. Ann Rev Neurosci. 17:185–218.

Arnaud L, Ballif BA, Forster E, Cooper JA. 2003. Fyn tyrosine kinase is a critical regulator of disabled-1 during brain development. Curr Biol. 13:9–17.

Blelloch R, Newman C, Kimble J. 1999. Control of cell migration during Caenorhabditis elegans development. Curr Opin Cell Biol. 11:608–613.

Bock HH, Herz J. 2003. Reelin activates SRC family tyrosine kinases in neurons. Curr Biol. 13:18–26.

Bystron I, Blakemore C, Rakic P. 2008. Development of the human cerebral cortex: Boulder Committee revisited. Nat Rev Neurosci. 9:110–122.

Caviness VS, Jr. 1982. Neocortical histogenesis in normal and reeler mice: a developmental study based upon [3H]thymidine autoradiography. Brain Res. 256:293–302.

Caviness VS, Jr., Rakic P. 1978. Mechanisms of cortical development: a view from mutations in mice. Ann Rev Neurosci. 1:297–326.

Caviness VS, Jr., Sidman RL. 1973. Time of origin or corresponding cell classes in the cerebral cortex of normal and reeler mutant mice: an autoradiographic analysis. J Comp Neurol. 148:141–151.

Chun JJ, Nakamura MJ, Shatz CJ. 1987. Transient cells of the developing mammalian telencephalon are peptide-immunoreactive neurons. Nature. 325:617–620.

Crandall JE, Jacobson M, Kosik KS. 1986. Ontogenesis of microtubule-associated protein 2 (MAP2) in embryonic mouse cortex. Brain Res. 393:127–133.
D'Arcangelo G, Miao GG, Chen SC, Soares HD, Morgan JI, Curran T. 1995. A protein related to extracellular matrix proteins deleted in the mouse mutant reeler. Nature. 374:719–723.
D'Arcangelo G, Miao GG, Curran T. 1996. Detection of the reelin breakpoint in reeler mice. Brain Res. 39:234–236.
De Carlos JA, O'Leary DD. 1992. Growth and targeting of subplate axons and establishment of major cortical pathways. J Neurosci. 12:1194–1211.
Del Rio JA, Martinez A, Auladell C, Soriano E. 2000. Developmental history of the subplate and developing white matter in the murine neocortex. Neuronal organization and relationship with the main afferent systems at embryonic and perinatal stages. Cereb Cortex. 10:784–801.
Denaxa M, Chan CH, Schachner M, Parnavelas JG, Karagogeos D. 2001. The adhesion molecule TAG-1 mediates the migration of cortical interneurons from the ganglionic eminence along the corticofugal fiber system. Development. 128:4635–4644.
Fukuda T, Kawano H, Ohyama K, Li HP, Takeda Y, Oohira A, Kawamura K. 1997. Immunohistochemical localization of neurocan and L1 in the formation of thalamocortical pathway of developing rats. J Comp Neurol. 382:141–152.
Goffinet AM. 1984. Events governing organization of postmigratory neurons: studies on brain development in normal and reeler mice. Brain Res. 319:261–296.
Gong S, Zheng C, Doughty ML, Losos K, Didkovsky N, Schambra UB, Nowak NJ, Joyner A, Leblanc G, Hatten ME, et al. 2003. A gene expression atlas of the central nervous system based on bacterial artificial chromosomes. Nature. 425:917–925.
Hanke JH, Gardner JP, Dow RL, Changelian PS, Brissette WH, Weringer EJ, Pollok BA, Connelly PA. 1996. Discovery of a novel, potent, and Src family-selective tyrosine kinase inhibitor. Study of Lck- and FynT-dependent T cell activation. J Biol Chem. 271:695–701.
Herz J, Bock HH. 2002. Lipoprotein receptors in the nervous system. Annu Rev Biochem. 71:405–434.
Hevner RF, Daza RA, Rubenstein JL, Stunnenberg H, Olavarria JF, Englund C. 2003. Beyond laminar fate: toward a molecular classification of cortical projection/pyramidal neurons. Dev Neurosci. 25:139–151.
Howell BW, Hawkes R, Soriano P, Cooper JA. 1997. Neuronal position in the developing brain is regulated by mouse disabled-1. Nature. 389:733–737.
Jones L, Lopez-Bendito G, Gruss P, Stoykova A, Molnar Z. 2002. Pax6 is required for the normal development of the forebrain axonal connections. Development. 129:5041–5052.
Jossin Y, Goffinet AM. 2007. Reelin signals through phosphatidylinositol 3-kinase and Akt to control cortical development and through mTor to regulate dendritic growth. Mol Cell Biol. 27:7113–7124.
Jossin Y, Ogawa M, Metin C, Tissir F, Goffinet AM. 2003. Inhibition of SRC family kinases and non-classical protein kinases C induce a reeler-like malformation of cortical plate development. J Neurosci. 23:9953–9959.
Kee Y, Hwang BJ, Sternberg PW, Bronner-Fraser M. 2007. Evolutionary conservation of cell migration genes: from nematode neurons to vertebrate neural crest. Genes Dev. 21:391–396.
Kostovic I, Rakic P. 1990. Developmental history of the transient subplate zone in the visual and somatosensory cortex of the macaque monkey and human brain. J Comp Neurol. 297:441–470.
Kuo G, Arnaud L, Kronstad-O'Brien P, Cooper JA. 2005. Absence of Fyn and Src causes a reeler-like phenotype. J Neurosci. 25:8578–8586.
McConnell SK, Ghosh A, Shatz CJ. 1994. Subplate pioneers and the formation of descending connections from cerebral cortex. J Neurosci. 14:1892–1907.
Meyer G, Goffinet AM. 1998. Prenatal development of reelin-immunoreactive neurons in the human neocortex. J Comp Neurol. 397:29–40.
Molnar Z, Metin C, Stoykova A, Tarabykin V, Price DJ, Francis F, Meyer G, Dehay C, Kennedy H. 2006. Comparative aspects of cerebral cortical development. Eur J Neurosci. 23:921–934.
Morante-Oria J, Carleton A, Ortino B, Kremer EJ, Fairen A, Lledo PM. 2003. Subpallial origin of a population of projecting pioneer neurons during corticogenesis. Proc Natl Acad Sci U S A. 100:12468–12473.
Nadarajah B, Brunstrom JE, Grutzendler J, Wong RO, Pearlman AL. 2001. Two modes of radial migration in early development of the cerebral cortex. Nat Neurosci. 4:143–150.
Nakamura N, Rabouille C, Watson R, Nilsson T, Hui N, Slusarewicz P, Kreis TE, Warren G. 1995. Characterization of a cis-Golgi matrix protein, GM130. J Cell Biol. 131:1715–1726.
Pinto-Lord MC, Evrard P, Caviness VS, Jr. 1982. Obstructed neuronal migration along radial glial fibers in the neocortex of the reeler mouse: a Golgi-EM analysis. Brain Res. 256:379–393.
Polleux F, Whitford KL, Dijkhuizen PA, Vitalis T, Ghosh A. 2002. Control of cortical interneuron migration by neurotrophins and PI3-kinase signaling. Development. 129:3147–3160.
Price DJ, Kennedy H, Dehay C, Zhou L, Mercier M, Jossin Y, Goffinet AM, Tissir F, Blakey D, Molnar Z. 2006. The development of cortical connections. Eur J Neurosci. 23:910–920.
Rakic P. 1972. Mode of cell migration to the superficial layers of fetal monkey cortex. J Comp Neurol. 145:61–84.
Richards LJ, Plachez C, Ren T. 2004. Mechanisms regulating the development of the corpus callosum and its agenesis in mouse and human. Clin Genet. 66:276–289.
Schaeren-Wiemers N, Gerfin-Moser A. 1993. A single protocol to detect transcripts of various types and expression levels in neural tissue and cultured cells: in situ hybridization using digoxigenin-labelled cRNA probes. Histochemistry. 100:431–440.
Shakir MA, Lundquist EA. 2005. Analysis of cell migration in Caenorhabditis elegans. Methods Mol Biol. 294:159–173.
Shi SH, Cheng T, Jan LY, Jan YN. 2004. APC and GSK-3beta are involved in mPar3 targeting to the nascent axon and establishment of neuronal polarity. Curr Biol. 14:2025–2032.
Solecki D, Govek EE, Tomoda T, Hatten ME. 2006. Neuronal polarity in CNS development. Genes Dev. 20:2639–2647.
Solecki DJ, Model L, Gaetz J, Kapoor TM, Hatten ME. 2004. Par6alpha signaling controls glial-guided neuronal migration. Nature neuroscience. 7:1195–1203.
Sym M, Robinson N, Kenyon C. 1999. MIG-13 positions migrating cells along the anteroposterior body axis of C. elegans. Cell. 98:25–36.
Tissir F, Goffinet AM. 2003. Reelin and brain development. Nat Rev Neurosci. 4:496–505.
Tomioka N, Osumi N, Sato Y, Inoue T, Nakamura S, Fujisawa H, Hirata T. 2000. Neocortical origin and tangential migration of guidepost neurons in the lateral olfactory tract. J Neurosci. 20:5802–5812.
Trommsdorff M, Gotthardt M, Hiesberger T, Shelton J, Stockinger W, Nimpf J, Hammer RE, Richardson JA, Herz J. 1999. Reeler/disabled-like disruption of neuronal migration in knockout mice lacking the VLDL receptor and ApoE receptor 2. Cell. 97:689–701.
Wang Y, Du D, Fang L, Yang G, Zhang C, Zeng R, Ullrich A, Lottspeich F, Chen Z. 2006. Tyrosine phosphorylated Par3 regulates epithelial tight junction assembly promoted by EGFR signaling. EMBO J. 25:5058–5070.
Wood J, Martin S, Price DJ. 1992. Evidence that the earliest generated cells of the murine cerebral cortex form a transient population in the subplate and marginal zone. Dev Brain Res. 66:137–140.
Xie Y, Skinner E, Landry C, Handley V, Schonmann V, Jacobs E, Fisher R, Campagnoni A. 2002. Influence of the embryonic preplate on the organization of the cerebral cortex: a targeted ablation model. J Neurosci. 22:8981–8991.
Zecevic N, Milosevic A, Rakic S, Marin-Padilla M. 1999. Early development and composition of the human primordial plexiform layer: an immunohistochemical study. J Comp Neurol. 412:241–254.
Zecevic N, Rakic P. 2001. Development of layer I neurons in the primate cerebral cortex. J Neurosci. 21:5607–5619.